

I would like to dedicate my thesis to my beloved parents, my inspiration and my epitome of hard work, honesty and happiness. They have always nurtured me with their unconditional love, trust and belief. My Sister and brother who always encourages me to do greater things in life.

To my dearest husband for always supporting me and giving me strength in hardest times of my life and to help me gather my will and move forward. This thesis is a gift of God who provides me strength, patience and perseverance.

..... Grateful and blessed

.....For my beautiful family

....My forever guiding light (Papa) this is for you



तेजपुर विश्वविद्यालय/TEZPUR UNIVERSITY
(संसद के अधिनियम द्वारा स्थापित केंद्रीय विश्वविद्यालय)
(A Central University established by an Act of
Parliament)

संकायाध्यक्ष का कार्यालय, शोध व विकास
Department of Molecular Biology and Biotechnology
तेजपुर-784028 :: असम / TEZPUR-784028 :: ASSAM



Dr. Venkata Satish Kumar Mattaparthi, M.Tech., Ph.D.,
Assistant Professor,
Department of Molecular Biology and Biotechnology


E-mail: venkata@tezu.ernet.in,
mvenkatasatishkumar@gmail.com
Phone no: 918811806866/03712-275443
Fax: 03712-267005/267006(O)

CERTIFICATE OF THE PRINCIPAL SUPERVISOR

This is to certify that the thesis entitled "*Computational investigation of membrane induced self-assembly and aggregation of α -Synuclein*" submitted to the School of Sciences, Tezpur University in partial fulfillment for the award of the degree of Doctor of Philosophy in Molecular Biology and Biotechnology is a record of original research work carried out by **Ms. Dorothy Das** under my personal supervision and guidance.

All helps received by her from various sources have been duly acknowledged. No part of this thesis has been reproduced elsewhere for award of any other degree.

Date: 24/10/2024
Place: Tezpur University, Tezpur


(Venkata Satish Kumar Mattaparthi)
Supervisor

Declaration

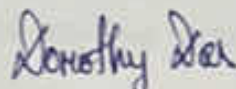
I hereby declare that the thesis entitled "*Computational investigation of membrane induced self-assembly and aggregation of α -Synuclein*" has been submitted to Tezpur University in the Department of Molecular Biology and Biotechnology under the School of Sciences for partial fulfillment for the award of the degree of Doctor of Philosophy in Molecular Biology and Biotechnology.

I am the sole author of this thesis. This is a true copy of an original work carried out by me including any required final revisions, as accepted by my examiners.

Further, I declare that no part of this work has been reproduced elsewhere for award of any other degree.

Date: 25/10/2024

Place: Tezpur University, Tezpur



Dorothy Das

Registration No.: TZ203952 of 2020

Declaration

I hereby declare that the thesis entitled “*Computational investigation of membrane induced self-assembly and aggregation of α -Synuclein*” has been submitted to Tezpur University in the Department of Molecular Biology and Biotechnology under the School of Sciences for partial fulfillment for the award of the degree of Doctor of Philosophy in Molecular Biology and Biotechnology.

I am the sole author of this thesis. This is a true copy of an original work carried out by me including any required final revisions, as accepted by my examiners.

Further, I declare that no part of this work has been reproduced elsewhere for award of any other degree.

Date:

Place: Tezpur University, Tezpur

Dorothy Das

Registration No.: TZ203952 of 2020



तेजपुर विश्वविद्यालय/TEZPUR UNIVERSITY
(संसद के अधिनियम द्वारा स्थापित केंद्रीय विश्वविद्यालय)
(A Central University established by an Act of
Parliament)

संकायाध्यक्ष का कार्यालय, शोध व विकास
Department of Molecular Biology and Biotechnology
तेजपुर-784028 :: असम / TEZPUR-784028 :: ASSAM



Dr. Venkata Satish Kumar Mattaparthi, M.Tech., Ph.D.,
Assistant Professor,
Department of Molecular Biology and Biotechnology

E-mail: venkata@tezu.ernet.in,
mvenkatasatishkumar@gmail.com
Phone no: 918811806866/03712-275443
Fax: 03712-267005/267006(O)

CERTIFICATE OF THE PRINCIPAL SUPERVISOR

This is to certify that the thesis entitled “*Computational investigation of membrane induced self-assembly and aggregation of α -Synuclein*” submitted to the School of Sciences, Tezpur University in partial fulfillment for the award of the degree of Doctor of Philosophy in Molecular Biology and Biotechnology is a record of original research work carried out by **Ms. Dorothy Das** under my personal supervision and guidance.

All helps received by her from various sources have been duly acknowledged.
No part of this thesis has been reproduced elsewhere for award of any other degree.

Date:

(Venkata Satish Kumar Mattaparthi)

Place: Tezpur University, Tezpur

Supervisor



TEZPUR UNIVERSITY
(A Central University established by an Act of
Parliament) Tezpur-784 028, Assam, India

CERTIFICATE OF THE EXTERNAL EXAMINER AND ODEC

This is to certify that the thesis entitled “*Computational investigation of membrane bound self-assembly and aggregation of α -Synuclein*” submitted by **Ms. Dorothy Das** to Tezpur University in the Department of Molecular Biology and Biotechnology under the School of Sciences in partial fulfillment of the requirement for the award of the degree of Doctor of Philosophy in Molecular Biology and Biotechnology has been examined by us on and found to be satisfactory.

The committee recommends for the award of the degree of Doctor of Philosophy.

Signature of:

Principal Supervisor

Date:

External examiner

Date:

Acknowledgement

I wish to express my heartfelt gratitude towards my supervisor, Dr. Venkata Satish Kumar Mattaparthi, for his guidance and support throughout my PhD journey. I feel blessed to be mentored by sir and understand the value of patience and wisdom. I will always be grateful to sir, for giving me a chance and for providing me immense support and freedom in conducting my research journey. During my doctoral research journey, I have always been encouraged and appreciated by sir that really encouraged me to work hard. My deep gratitude goes to him for all his dedication and steadiness during the writing of the thesis. I thank him for every wisdom.

I would also like to thank the Head, Department of MBBT, Tezpur University, and my Doctoral Committee members – Prof. Manabendra Mandal and Dr. Rupak Mukhopadhyay, Head of the Department of MBBT, Tezpur University, for their insight, comments, and valuable suggestions during my Ph.D. tenure.

I would like to acknowledge all other faculty members in the Department of MBBT, Tezpur University for their help and encouragement and the non-teaching staffs of the Department for their technical support. I would like to take this opportunity to thank Tezpur University for providing me with the state-of-the-art infrastructure and facilities for advanced research.

I would like to extend my gratitude to financial support provided by Department of Science and Engineering Research Board (SERB) and Tezpur University for my research work and high facility equipments HPCC (High performance computing cluster).

No word would be enough for expressing my gratitude towards lab mates in MOMO Lab: Airy Sanjeev, Mridusmita Kakati, Sushmita di, Pundarikaksha dada, Priyanka, Chaine and Babli for supporting me in many occasions during this work and for all the time we spent together. Heartfelt thanks to all the project students (Navamallika, Krishna, Pallav, Priya, Ambika, Barsha, Hrishikesh, Ayon and Debatri) for their help and support.

I would like to express my gratitude to Dr. Priyam Bharadwaz, J. Heyrovsky Institute of Physical Chemistry, Czech Academy of Sciences, Prague, Czech Republic for running DFT calculations and optimization of small molecule inhibitors for inhibition studies.

Above ground, my biggest thanks of all goes to my Papa and Maa, my siblings (Gayatri Baa and Jayanta Dada), my husband Koushik and my loving father-in-law and mother-in law for their fulltime support and unconditional love and for giving me a contended life with full of joy and happiness.

Regards,

Dorothy Das

List of Figures

Figure No.	Chapter 1	Page No.
1.1	The involvement of Lipid Membranes in α -Syn Aggregation and its Association with PD	2
Figure No.	Chapter 2	Page No.
2.1	Schematic representation of IDP. '1' indicates native structure, '2' showed intermediate structure and '3' indicated ordered aggregates	8
2.2	Schematic representation of different states of folding, unfolding, and aggregation of protein to attain a stable state	10
2.3	Schematic representation of Physiological and pathological conformations of α -Syn	12
2.4	Schematic representation of transmission of chemical synaptic in the presynaptic cell	15
2.5	Diagrammatic representation of dopamine levels in a normal and PD affected neurons	15
2.6	Representation of motor and non-motor symptoms of PD	16
2.7	Structure of α -Syn protein showing different domains, mutational sites and phosphorylation sites linked to familial PD	19
2.8	Events of α -Syn monomers followed by pathogenicity of PD	19
2.9	3-D Structure of α -Syn (1XQ8 PDB ID)	21
2.10	Point missense mutations of α -Syn protein in membrane bound state	25
Figure No.	Chapter 3	Page No.
3.1	Diagrammatic illustration of the main contribution to the potential energyfunction	37
3.2	The two dimensional projection of Periodic boundary conditions. The simulation cell (dark color) is surrounded by translated copies of itself (light color)	41
3.3	Schematic representation of TIP3P water model	43
3.4	Schematic representation of the steps involved in MD simulation	44
3.5	A schematic representation of the Different phases of a molecule during minimization of its energy	45
3.6	The quadratic function $f(x) = x^T (2 \ 11 \ 6)x$ is subjected to three different approaches. Plots on the contour plot of demonstrate different iterations of the techniques	47
3.7	A line search is used to locate the minimum in the function in the direction of the gradient	47
3.8	The structure-based and template-based blind docking algorithms performed by CB-Dock2 server integration	55
3.9	Wiring diagram showing secondary structures present in α -Syn protein (1XQ8 pdb). Helices are labelled as H1, H2, H3, H4, H5, and H6	57
3.10	Surface topology diagram showing number of helices, beta turns, and gamma turns in α -Syn protein (1XQ8 pdb)	57

List of Figures

3.11	Ligplot analysis showing hydrophobic interaction, hydrogen bonds between α -Syn protein (1XQ8 pdb) and ligand molecule (NPT100-18A)	58
3.12	Flowchart of the main steps of FastDRH server to calculate the hotspot prediction thereby calculate the binding free energy analysis	60
3.13	The primary CASTp server user interface. (A) The panel in the pocket and (B) sequence panels	62
3.14	Construction of α -Syn mutants using UCSF Chimera software	68
Chapter 4		
Figure No.	Chapter 4	Page No.
4.1	Area per lipid analysis for α -Syn as a function of simulation time	74
4.2	Membrane thickness analysis for α -Syn as a function of simulation time	75
4.3	Electron density profile analysis for α -Syn as a function of simulation time	76
4.4	Electron density profile analysis for each region of α -Syn as a function of simulation time	76
4.5	RMSD analysis of α -Syn as a function of simulation time	77
4.6	RMSD analysis for each region of α -Syn as a function of simulation time	77
4.7	PCA followed by 2D (left) and 3D (middle) free energy landscapes (FEL) analysis of α -Syn. X, Y, and Z indicate PC1, PC2, and free energy, respectively. In the energy well, '1', reflect the global minimum of α -Syn. Colour-coded mode was used to correlate structural conformations and free energy of α -Syn. The right-most panel shows energy wells with global free energy minima for α -Syn	78
4.8	RMSF analysis of α -Syn as a function of simulation time	78
4.9	DSSP plot of secondary Structural content of α -Syn during MD simulation obtained from Kabsch and Sander algorithm	79
4.10	Secondary structure Probability score of α -Syn during MD simulation	80
4.11	Conformational snapshots of α -Syn during MD simulation	81
4.12	Intermolecular hydrogen bond analysis of α -Syn during MD simulation	82
4.13	Intermolecular hydrogen bond analysis of different regions of α -Syn during MD simulation	83
4.14	Distance analysis of α -Syn during MD simulation as a function of simulation time	86
Chapter 5a		
Figure No.	Chapter 5a	Page No.
5a.1	Comparative MD analyses of (A) RMSD, (B) Rg, (C) RMSF and (D) SASA, for α -Syn in different concentration of ethanol	92

List of Figures

5a.2	Probability score of secondary structure for each residue in α -Syn in 0%, 5%, 10%, 20%, 50% and 100% ethanol concentration	93
5a.3	Time evolution of Secondary structure of α -Syn in presence of 0%, 5%, 10%, 20%, 50% and 100% ethanol	95
5a.4	Snapshots of α -Syn conformers in presence of 0%, 5%, 10%, 20%, 50% and 100% ethanol during the time course of simulation	95
Chapter 5b		
Figure No.		Page No.
5b.1	RMSD plot of α -Syn during MD simulation as function of simulation time	100
5b.2	(A) Density, (B) Pressure, (C) Energy plots and (D) Temperature of α -Syn as a function of simulation time	101
5b.3	Radius of Gyration analysis for α -Syn as a function of simulation time	103
5b.4	SASA analysis for α -Syn as function of simulation time	103
5b.5	Binding pocket analysis for the conformers of α -Syn having (A) Lower R_g values (B) Moderate R_g values. (C) Higher R_g values	105
5b.6	The evolution of secondary structure evaluated using DSSP is shown for α -Syn. Y-axis depicts residues and X-axis depicts time frames during the course of MD simulation. The secondary structure components of α -Syn are color-coded as shown in the panel.	107
Chapter 6		
Figure No.		Page No.
6.1	(A) Pressure (B) Temperature and (C) Energy plots of A30G α -Syn as a function of simulation time	119
6.2	Graphical illustration of membrane bound A30G α -Syn built using CHARMM GUI server. For better visuals, ions and water box was not included. The snapshots are generated using UCSF CHIMERA 1.14	121
6.3	(A) Area per lipid (upper and lower) layer analysis for membrane bound A30G α -Syn during simulation time period of 100 ns (B) the average membrane thickness in angstroms plotted with respect to simulation time period of 100 ns	123
6.4	Electron Density Profile (A) of the membrane bound A30G α -Syn and (B) each component of A30G α -Syn	124
6.5	Snapshots of (A) membrane bound A30G α -Syn and (B) membrane bound (hidden) A30G α -Syn after simulation time period of 100 ns	126
6.6	Snapshots of A30G α -Syn as a monomer in free solution after simulation time period of 100 ns. A30G α -Syn backbone is represented as N-helix (pink), turn (blue) and C-helix (green)	126

List of Figures

6.7	Snapshots of A30G α -Syn conformations on its interaction with the lipid membrane after 100 ns of simulated dynamics	127
6.8	Snapshot of membrane bound A30G α -Syn showing two (i, i+2) paired lysine residues in opposite direction along the lipid bilayer surface	127
6.9	RMSD analysis of N-terminal, NAC region and C-terminal of (A) membrane bound A30G α -Syn (B) A30G α -Syn in free solution. (C) Comparison of C α RMSD for membrane bound A30G α -Syn and in free solution during MD simulation of 100 ns	128
6.10	Radius of gyration analysis of (A) membrane bound state A30G α -Syn and (B). A30G α -Syn in free solution during simulation time	129
6.11	RMSF analysis of (A) membrane bound A30G α -Syn and (B) A30G α -Syn in free monomeric form in solution during simulation time period of 100 ns	130
6.12	Secondary structural analysis of (A) A30G α -Syn in membrane bound form (B) A30G α -Syn in free monomer form	131
6.13	Secondary structure Probability score of (A) membrane bound A30G α -Syn and (B) A30G α -Syn in free monomer form	131
6.14	Surface topology analysis of (A) membrane bound A30G α -Syn and (B) A30G α -Syn in free monomer form during the simulation time	132
6.15	List of helices observed in membrane bound A30G α -Syn during the simulation time	133
6.16	List of helices observed in A30G α -Syn in free solution during the simulation time	133
6.17	The number of intermolecular hydrogen bonds between N-terminal, NAC region and C-terminal of membrane bound A30G α -Syn during MD simulation of 100 ns	134
6.18	The number of intermolecular hydrogen bonds between membrane bilayer and (A) N-terminal, (B) NAC region and (C) C-terminal of A30G α -Syn during MD simulation of 100 ns	135
6.19	The number of intramolecular hydrogen bonds within N-terminal, NAC region and C terminal of (A) A30G α -Syn in membrane bound form and (B) in free form during MD simulation time. The number of intramolecular hydrogen bonds within N-helix, Turn and C-helix of (C) A30G α -Syn in membrane bound form and (D) in free form during MD simulation time	139

List of Figures

6.20	Distance analysis between N-terminal and C-terminal domains of (A) membrane bound A30G α -Syn and (B) A30G α -Syn as a free monomer in solution	140
6.21	Helical bending at position Glycine 67/68 during the simulation period of 100 ns. The color scheme is as follows: (A) A30G α -Syn in lipid-bound state (blue) and (B) free monomer state (red)	141
6.22	Torsion angle analysis for the A30G α -Syn in (A-B) membrane bound form and (C-D) free monomeric form for the residues 26 and 28 as a function of simulation time	142
6.23	Snapshots showing different conformations of the (A) membrane bound A30G α -Syn and (B) A30G α -Syn in free monomer form during the simulation time	142
6.24	PONDR VLXT score calculated for (A) WT α -Syn and (B) A30G α -Syn in free monomer form during the simulation time	144
Figure No. Chapter 7 Page No.		
7.1	Area per lipid analysis of A30P, A53E, A53T, E46K, G51D and H50Q α -Syn mutants	151
7.2	Membrane thickness analysis of membrane bound α -Syn mutants as a function of simulation time	152
7.3	Electron density profile analysis of each component of (A) A30P, (B) A53E, (C) A53T, (D) E46K, (E) G51D and (F) H50Q α -Syn mutants	153
7.4	Electron density profile analysis of different regions of (A) A30P, (B) A53E, (C) A53T, (D) E46K, (E) G51D and (F) H50Q α -Syn mutants	154
7.5	RMSD analysis of membrane bound α -Syn mutants as a function of simulation time	155
7.6	RMSF analysis of membrane bound α -Syn mutants as a function of simulation time	156
7.7	Intermolecular Hydrogen bond analysis between (A) A30P, (B) A53E, (C) A53T, (D) E46K, (E) G51D and (F) H50Q α -Syn mutants and lipid membrane	157
7.8	Conformational snapshots of (A) membrane bound A30P α -Syn and (B) membrane hidden as a function of simulation time	169
7.9	Conformational snapshots of (A) membrane bound A53E α -Syn and (B) membrane hidden as a function of simulation time	170
7.10	Conformational snapshots of (A) membrane bound A53T α -Syn and (B) membrane hidden as a function of simulation time	171

List of Figures

7.11	Conformational snapshots of (A) membrane bound E46K α -Syn and (B) membrane hidden as a function of simulation time	171
7.12	Conformational snapshots of (A) membrane bound G51D α -Syn and (B) membrane hidden as a function of simulation time	172
7.13	Conformational snapshots of (A) membrane bound H50Q α -Syn and (B) membrane hidden as a function of simulation time	173
7.14	DSSP plot of (A) A30P, (B) A53E, (C) A53T, (D) E46K, (E) G51D and (F) H50Q α -Syn mutants using Kabsch and sander algorithm	174
7.15	Percentage secondary probability score of (A) A30P, (B) A53E, (C) A53T, (D) E46K, (E) G51D and (F) H50Q α -Syn mutants and lipid membrane	175
7.16	Distance analysis between N-terminal and C-terminal of membrane bound α -Syn mutants as a function of simulation time	176
Chapter 8a		
Figure No.	Chapter 8a	Page No.
8a.1	B3LYP+D3/def2-TZVP (/CPCM) calculated optimized structure of inhibitors (NPT100-18A and NPT200-11) considered in this study	182
8a.2	Schematic representation for the formation of docked complexes (α -Syn +NPT100-18A and α -Syn +NPT200-11)	183
8a.3	(A) Electron density plot of B3LYP+D3/def2-TZVP (/CPCM) calculated inhibitors (NPT100-18A and NPT200-11) according to the electrostatic potential map (ESP). Electrostatic potential energy data is estimated as a color spectrum, with red as the lowest electrostatic negative charge and blue as the highest to convey the varying intensities of the electrostatic potential maps. (B) and (C) represent the energies (in eV) of first five highest occupied (HOMO, HOMO-1, HOMO-2, HOMO-3, and HOMO-4) and lowest unoccupied (LUMO, LUMO+1, LUMO+2, LUMO+3 and LUMO+4) frontier molecular orbitals of NPT100-18A and NPT200-11 respectively in B3LYP+D3/def2-TZVP (/CPCM) level of theory	187
8a.4	Area per lipid analysis for (A) NPT100-18A inhibitor α -Syn and (B) NPT200-11 inhibitor α -Syn	188
8a.5	Membrane thickness analysis of for (A) NPT100-18A associated membrane bound α -Syn and (B) NPT200-11 associated membrane bound α -Syn during MD simulation	189

List of Figures

8a.6	Electron density profile of (A) NPT100-18A inhibitor and (B) NPT200-11 inhibitor attached to the α -Syn after the simulation	191
8a.7	Electron density profile of (A) inhibitor NPT100-18A- α -Syn and (B) inhibitor NPT200-11 α -Syn complexes after the simulation of 100 ns	191
8a.8	Electron density profile of (A) inhibitor NPT100-18A (B) inhibitor NPT200-11 in association with membrane bilayer after the simulation of 100 ns	191
8a.9	3-D snapshot of membrane bound α -Syn in presence of inhibitor NPT100-18A during MD simulation	192
8a.10	3-D snapshot of membrane bound α -Syn in presence of inhibitor NPT200-11 during MD simulation	192
8a.11	Ligplot analysis showing the interactions between NPT100-18A inhibitor and membrane bilayer during MD simulation	193
8a.12	Ligplot analysis showing the interactions between NPT200-11 inhibitor and membrane bilayer during MD simulation	194
8a.13	Snapshots of conformational changes observed in membrane bound α -Syn in presence NPT100-18A inhibitor	195
8a.14	Snapshots of conformational changes observed in membrane bound α -Syn in presence NPT200-11 inhibitor	196
8a.15	Snapshots of (A) α -Syn (B) α -Syn+NPT100-18A and (C) α -Syn+NPT200-11 showing N-terminal (residue 1-37) in green color and NAC region (residues 45-95) in red color after MD simulation run of 100 ns	196
8a.16	RMSD analysis of (A) inhibitor (NPT100-18A and NPT200-11) α -Syn complexes (B) RMSD analysis of inhibitors (NPT100-18A and NPT200-11) after the simulation of 100 ns	197
8a.17	RMSD analysis of (A) N-terminal (B) NAC region and (C) C-terminal of α -Syn apo and inhibitor (NPT100-18A and NPT200-11) complexes	198
8a.18	PCA followed by 2D (left) and 3D (middle) free energy landscapes (FEL) analysis of α -Syn in the presence of (A) inhibitors NPT100-18A and (B) NPT200-11 respectively. X, Y, and Z indicate PC1, PC2, and free energy, respectively. In the energy well, '2', and '3' reflect the global minimum of α -Syn in the presence (A and B) of inhibitors NPT100-18A and NPT200-11. Colour-coded mode was used to correlate structural conformations and free energy of α -Syn in the presence of inhibitors NPT100-18A and NPT200-11. The right-most panel shows energy wells	199

List of Figures

	with global free energy minima for α -Syn in the presence of inhibitors	
8a.19	RMSF analysis of membrane-bound α -Syn- inhibitors (NPT100-18A and NPT200-11) complexes after the simulation of 100 ns	200
8a.20	Distance analysis between (A) N-terminal and NAC region and (B) N-terminal and C-terminal and (C) NAC region and C-terminal of α -Syn in presence and absence of peptidomimetic inhibitors	201
8a.21	DSSP plot of secondary Structural content of α -Syn in the presence of inhibitor (A) NPT100-18A and (B) NPT200-11 complex during MD simulation obtained from Kabsch and Sander algorithm	203
8a.22	Secondary structure Probability score of (A) N-terminal (B) NAC region and (C) C-terminal of α -Syn in presence of NPT100-18A inhibitor	203
8a.23	Secondary structure Probability score of (A) N-terminal (B) NAC region and (C) C-terminal of α -Syn in presence of NPT200-11 inhibitor	203
8a.24	The number of intermolecular Hydrogen bond analysis between membrane bilayer and all the regions of (A) NPT100-18A and (B) NPT200-11 complexes	205
Chapter 8b		
Figure No.	Chapter 8b	Page No.
8b.1	B3LYP + D3/Def2TZVP, CPCM calculated singlet optimized structure of squalamine complex considered in this study	216
8b.2	B3LYP + D3/Def2TZVP, CPCM calculated singlet optimized structure of trodusquemine complex considered in this study.	216
8b.3	(A) Energies (in eV) of first five highest occupied (HOMO, HOMO-1, HOMO-2, HOMO-3, and HOMO-4) and lowest unoccupied (LUMO, LUMO+1, LUMO+2, LUMO+3 and LUMO+4) frontier molecular orbitals of squalamine complex calculated in B3LYP+D3/def2-TZVP (/CPCM) level of theory. (B) Calculated electron density plot from electrostatic potential map (ESP) for squalamine complex at B3LYP+D3/def2-TZVP (/CPCM) level of theory	219
8b.4	(A) Energies (in eV) of first five highest occupied (HOMO, HOMO-1, HOMO-2, HOMO-3, and HOMO-4) and lowest unoccupied (LUMO, LUMO+1, LUMO+2, LUMO+3 and LUMO+4) frontier molecular orbitals of trodusquemine complex calculated in B3LYP+D3/def2-TZVP (/CPCM) level of theory. (B) Calculated electron density plot from electrostatic potential map (ESP) for trodusquemine complex at B3LYP+D3/def2-TZVP (/CPCM) level of theory.	219

List of Figures

8b.5	Conformational snapshots of membrane-bound α -Syn in the presence of inhibitor Squalamine during MD simulation	222
8b.6	Conformational snapshots of membrane-bound α -Syn in the presence of inhibitor Squalamine during MD simulation (membrane hidden)	223
8b.7	3-D snapshot of membrane bound α -Syn in presence of inhibitor squalamine during MD simulation	223
8b.8	Conformational snapshots of membrane-bound α -Syn in the presence of inhibitor trodusquemine prior to MD simulation	224
8b.9	Ligplot analysis of membrane-bound α -Syn in the presence of inhibitor Squalamine during MD simulation	225
8b.10	Ligplot analysis of the interaction between membrane bilayer and inhibitor Squalamine at different time intervals during MD simulation	226
8b.11	Ligplot analysis of membrane-bound α -Syn in the presence of inhibitor Trodusquemine prior to the MD simulation	226
Figure No.		
Chapter 9		
Page No.		
9.1	Truncation of CTD of α -Syn (1-99 and 1-108) followed by MD simulation	235
9.2	Area per Lipid analysis of truncated CTD α -Syn (1-99 and 1-108) from the MD simulation trajectories	237
9.3	Electron Density Profile analysis of each component of truncated CTD α -Syn (A) (1-99) and (B) (1-108) from the MD simulation trajectories of 100 ns	238
9.4	Electron Density Profile analysis of each region of truncated CTD α -Syn (A) (1-99) and (B) (1-108) from the MD simulation trajectories of 100 ns	238
9.5	RMSD analysis of all the C α atoms of truncated CTD α -Syn (A) (1-99) and (B) (1-108) from the MD simulation trajectories of 100 ns	239
9.6	RMSD analysis of N-terminal and NAC region of truncated CTD α -Syn (A) (1-99) and (B) (1-108) from the MD simulation trajectories of 100 ns	240
9.7	RMSF analysis of all the C α atoms of truncated CTD α -Syn (A) (1-99) and (1-108) from the MD simulation trajectories of 100 ns	240
9.8	DSSP plot of secondary Structural content of truncated CTD α -Syn (A) (1-99) and (B) (1-108) during MD simulation obtained from Kabsch and Sander algorithm	241
9.9	Secondary structure Probability Score of N-terminal and NAC region of truncated CTD α -Syn (A) (1-99) and (B) (1-108) from the MD simulation trajectories of 100 ns	241
9.10	Radius of gyration analysis of truncated CTD α -Syn (A) (1-99) and (B) (1-108) from the MD simulation trajectories of 100 ns	242
9.11	Intermolecular hydrogen bond analysis between the NAC region of truncated CTD α -Syn (A) (1-99) and	243

List of Figures

	(B) (1-108) and Lipid membrane from the MD simulation trajectories of 100 ns	
9.12	Principle Component Analysis followed Gibbs free energy landscape (FEL) plot of truncated CTD α -Syn (A) (1-99) and (B) (1-108) from the MD simulation trajectories of 100 ns. (1) and (2) indicates lowest energy structure, along with the two principal eigenvectors (PC1 and PC2). The black region depicts conformations with lower energy, the red color signifies the meta-stable states and the blue corresponds to conformations having high energy	249
9.13	Conformational snapshots of truncated CTD (1-99) (A) α -Syn in association with lipid membrane and (B) membrane hidden	251
9.14	Conformational snapshots of truncated CTD (1-108) (A) α -Syn in association with lipid membrane and (B) membrane hidden	252
9.15	Distance Analysis of truncated CTD α -Syn (1-99) and (1-108) from the MD simulation trajectories of 100 ns	253
Figure No.		
Chapter 10		
Page No.		
10.1	Schematic representation of the phosphorylation of α -Syn at pY39, pS87 and pS129 followed by MD simulation	261
10.2	Area per lipid bilayer of the phosphorylated α -Syn (A) pY39, (B) pS87 and (C) pS129 during MD simulation	264
10.3	Membrane thickness of the phosphorylated α -Syn (A) pY39, (B) pS87 and (C) pS129 during MD simulation	265
10.4	Electron density plots of the phosphorylated α -Syn (A) pY39, (B) pS87 and (C) pS129 during MD simulation	266
10.5	Electron density plots of each component of the phosphorylated α -Syn (A) pY39, (B) pS87 and (C) pS129 during MD simulation	266
10.6	RMSD analysis of phosphorylated α -Syn (A) pY39, (B) pS87 and (C) pS129 during MD simulation of 100 ns	268
10.7	PCA followed by 2D and 3D free energy landscapes (FEL) analysis of (A) pY39, (B) pS87 and (C) pS129 α -Syn. X, Y, and Z indicate PC1, PC2, and free energy, respectively. In the energy well, '1' reflects the global minimum of all the phosphorylated α -Syn structures	269
10.8	RMSF analysis of phosphorylated α -Syn (A) pY39, (B) pS87 and (C) pS129 during MD simulation of 100 ns	270
10.9	Radius of gyration analysis of phosphorylated α -Syn (A) pY39, (B) pS87 and (C) pS129 during MD simulation of 100 ns	271
10.10	DSSP plot of the phosphorylated α -Syn (A) pY39, (B) pS87 and (C) pS129 using Kabsch and Sander Algorithm	273

List of Figures

10.11	(A) Conformational snapshots of phosphorylated pS129 α -Syn throughout the MD simulation time and (B) Ramachandran plot (ϕ , ψ) showing right-handed (α_R) and left-handed (α_L) helical regions	274
10.12	Conformational Snapshots of the phosphorylated (pY39) α -Syn (A) membrane hidden and (B) membrane bound as a function of simulation time	275
10.13	Conformational Snapshots of the phosphorylated (pS87) α -Syn (A) membrane hidden and (B) membrane bound as a function of simulation time	276
10.14	Conformational Snapshots of the phosphorylated (pS129) α -Syn (A) membrane hidden and (B) membrane bound as a function of simulation time	277
10.15	Intermolecular hydrogen bond analysis between (A) N-terminal, (B) NAC region and (C) C-terminal of the phosphorylated α -Syn pY39 and lipid membrane during MD simulation	278
10.16	Intermolecular hydrogen bond analysis between (A) N-terminal, (B) NAC region and (C) C-terminal of the phosphorylated α -Syn pS87 and lipid membrane during MD simulation	278
10.17	Intermolecular hydrogen bond analysis between (A) N-terminal, (B) NAC region and (C) C-terminal of the phosphorylated α -Syn pS129 and lipid membrane during MD simulation	279
10.18	Intramolecular of the phosphorylated α -Syn (A) N-terminal, (B) NAC region, and (C) C-terminal of the phosphorylated α -Syn pY39 during MD simulation	287
10.19	Intramolecular of the phosphorylated α -Syn (A) N-terminal, (B) NAC region, and (C) C-terminal of the phosphorylated α -Syn pS87 during MD simulation	288
10.20	Intramolecular of the phosphorylated α -Syn (A) N-terminal, (B) NAC region, and (C) C-terminal of the phosphorylated α -Syn pS129 during MD simulation	289
10.21	Distance analysis of the phosphorylated α -Syn (A) pY39, (B) pS87 and (C) pS129 during MD simulation	291

List of Tables

Table No.	Chapter 2	Page No.
2.1	Table showing recent research advancements in α -Syn associated PD pathology	22
2.2	Comparison of the consequences of several early onset mutations in the SNCA gene with respect to the WT protein, including age of onset, lipid binding, and fibril development rates	25
Chapter 4		
Table No.	Chapter 4	Page No.
4.1	Secondary structural content of WT α -Syn during MD simulation	79
4.2	Intermolecular Hydrogen bond analysis of membrane bound α -Syn complex during the MD simulation of 100 ns with membrane bilayer as acceptor and α -Syn as donor	83
4.3	Intermolecular Hydrogen bond analysis of membrane bound α -Syn complex during the MD simulation of 100 ns with membrane bilayer as donor and α -Syn as acceptor	84
Chapter 5a		
Table No.	Chapter 5a	Page No.
5a.1	Secondary structure content of α -Syn in 0%, 5%, 10%, 20%, 50% and 100% ethanol	94
5a.2	Diffusion Coefficient values of α -Syn in different concentrations of ethanol	96
Chapter 5b		
Table No.	Chapter 5b	Page No.
5b.1	R_g , SASA and Number of binding pockets for the screened conformers of α -Syn having lower, middle and higher R_g values	105
5b.2	Secondary structure content and the Number of Binding Pockets for the conformers of α -Syn having lower, middle and higher R_g values	107
5b.3	Binding Pocket Information for all the screened conformers of α -Syn	108
Chapter 6		
Table No.	Chapter 6	Page No.
6.1	Intermolecular Hydrogen bond analysis of membrane bound A30G mutant complex during the MD simulation of 100 ns with membrane bilayer as acceptor and A30G mutant as donor	135
6.2	Intermolecular Hydrogen bond analysis of membrane bound A30G mutant complex during the MD simulation of 100 ns with A30G mutant as acceptor and membrane bilayer as donor	136
6.3	$\Delta\Delta G$ values upon single point mutation (A30G) in α -Syn	143
6.4	SIFT analysis to predict the tolerance of a single mutation A30G on WT α -Syn	143
Chapter 7		
Table No.	Chapter 7	Page No.
7.1	List of mutation of α -Syn protein and its structure	149
7.2	Intermolecular Hydrogen bond analysis of membrane bound A30P α -Syn complex during the MD simulation	157

List of Tables

	of 100 ns with membrane bilayer as acceptor and A30P α -Syn as donor	
7.3	Intermolecular Hydrogen bond analysis of membrane bound A30P α -Syn complex during the MD simulation of 100 ns with A30P α -Syn as acceptor and membrane bilayer as donor	158
7.4	Intermolecular Hydrogen bond analysis of membrane bound A53E α -Syn complex during the MD simulation of 100 ns with membrane bilayer as acceptor and A53E α -Syn as donor	159
7.5	Intermolecular Hydrogen bond analysis of membrane bound A53E α -Syn complex during the MD simulation of 100 ns with A53E α -Syn as acceptor and membrane bilayer as donor	160
7.6	Intermolecular Hydrogen bond analysis of membrane bound A53T α -Syn complex during the MD simulation of 100 ns with membrane bilayer as acceptor and A53T α -Syn as donor	161
7.7	Intermolecular Hydrogen bond analysis of membrane bound A53T α -Syn complex during the MD simulation of 100 ns with A53T α -Syn as acceptor and membrane bilayer as donor	162
7.8	Intermolecular Hydrogen bond analysis of membrane bound E46K α -Syn complex during the MD simulation of 100 ns with membrane bilayer as acceptor and E46K α -Syn as donor	163
7.9	Intermolecular Hydrogen bond analysis of membrane bound E46K α -Syn complex during the MD simulation of 100 ns with E46K α -Syn as acceptor and membrane bilayer as donor	164
7.10	Intermolecular Hydrogen bond analysis of membrane bound G51D α -Syn complex during the MD simulation of 100 ns with membrane bilayer as acceptor and G51D α -Syn as donor	165
7.11	Intermolecular Hydrogen bond analysis of membrane bound G51D α -Syn complex during the MD simulation of 100 ns with G51D α -Syn as acceptor and membrane bilayer as donor	165
7.12	Intermolecular Hydrogen bond analysis of membrane bound H50Q α -Syn complex during the MD simulation of 100 ns with membrane bilayer as acceptor and H50Q α -Syn as donor	166
7.13	Intermolecular Hydrogen bond analysis of membrane bound H50Q α -Syn complex during the MD simulation of 100 ns with H50Q α -Syn as acceptor and membrane bilayer as donor	167
7.14	Secondary structural content of all the α -Syn mutants during MD simulation	176
Table No.	Chapter 8a	Page No.
8a.1	Energies (in eV) of the first five highest occupied (HOMO, HOMO-1, HOMO-2, HOMO-3, and HOMO-4) and lowest unoccupied (LUMO, LUMO+1, LUMO+2, LUMO+3 and LUMO+4) frontier molecular	186

List of Tables

	orbitals of NPT100-18 and NPT200-11 respectively in B3LYP+D3/def2-TZVP (/CPCM) level of theory	
8a.2	Calculated values of nucleophilicity (N, eV) and electrophilicity (ω , eV) indices, ionization potential (IP, in kcal/mol), electron affinity (EA, in kcal/mol) and HOMO-LUMO band gap ($\Delta E_{\text{HOMO-LUMO}}$, in kcal/mol) for NPT100-18A and NPT200-11	187
8a.3	Secondary structural content of the α -Syn in presence of inhibitors (NPT100-18A and NPT200-11) during MD simulation	202
8a.4	Intermolecular Hydrogen bond analysis of membrane bound NPT100-18A- α -Syn complex during the MD simulation of 100 ns with membrane bilayer as acceptor and α -Syn in presence of NPT100-18A inhibitor as donor	205
8a.5	Intermolecular Hydrogen bond analysis of membrane bound NPT100-18A- α -Syn complex complex during the MD simulation of 100 ns with α -Syn in presence of NPT100-18A inhibitor as acceptor and membrane bilayer as donor	207
8a.6	Intermolecular Hydrogen bond analysis of membrane bound NPT200-11- α -Syn complex during the MD simulation of 100 ns with membrane bilayer as acceptor and α -Syn in presence of NPT200-11 as donor	208
8a.7	Intermolecular Hydrogen bond analysis of membrane bound NPT200-11- α -Syn complex during the MD simulation of 100 ns with α -Syn in presence of NPT200-11 inhibitor as acceptor and membrane bilayer as donor	209
8a.8	Binding free energies (kcal/mol) and its derived components of α -Syn protein and inhibitor (NPT100-18A and NPT200-11) complexes obtained using FastDRH server	210
Table No.	Chapter 8b	Page No.
8b.1	Calculated values of nucleophilicity (N, eV) and electrophilicity (ω , eV) indices, ionization potential (IP, in kcal/mol), electron affinity (EA, in kcal/mol) and HOMO-LUMO band gap ($\Delta E_{\text{HOMO-LUMO}}$, in kcal/mol) for squalamine and trodusquemine molecules	220
8b.2	Predicted binding sites of the α -Syn+Squalamine complex using CB-docking2 server including Molecular Docking Score, cavity volume and contact residues	220
8b.3	Predicted binding sites of the α -Syn+Trodusquemine complex using CB-docking2 server including Molecular Docking Score, cavity volume and contact residues.	221
8b.4	Secondary Structural content of α -Syn+squalamine after the simulation time using YASARA software	227
8b.5	Secondary Structural content of α -Syn+trodusquemine at the initial MD simulation using YASARA software	227
8b.6	Binding free energies (kcal/mol) and its derived components of α -Syn protein and inhibitor molecules	228

List of Tables

	(squalamine and trodusquemine) complex obtained using FastDRH server	
8b.7	List of atom-atom interactions within the α -Syn+Squalamine interface from the ESBRI server	229
8b.8	List of atom-atom interactions within the α -Syn+Trodusquemine interface from the ESBRI server	229
Chapter 9		
Table No.	Chapter 9	Page No.
9.1	Secondary Structural details of the truncated CTD α -Syn showing the percentage of secondary contents and similarity threshold as predicted by SOPMA (Self-Optimized Prediction Method with Alignment)	241
9.2	Intermolecular Hydrogen bond analysis of membrane-bound truncated CTD α -Syn (1-99) during the MD simulation of 100 ns with membrane bilayer as acceptor and truncated CTD α -Syn (1-99) as donor	243
9.3	Intermolecular Hydrogen bond analysis of membrane bound truncated CTD α -Syn (1-99) during the MD simulation of 100 ns with membrane bilayer as donor and truncated CTD α -Syn (1-99) as acceptor	245
9.4	Intermolecular Hydrogen bond analysis of membrane bound truncated CTD α -Syn (1-108) during the MD simulation of 100 ns with membrane bilayer as acceptor and truncated CTD α -Syn (1-108) as donor	246
9.5	Intermolecular Hydrogen bond analysis of membrane bound truncated CTD α -Syn (1-108) during the MD simulation of 100 ns with membrane bilayer as donor and truncated CTD α -Syn (1-108) as acceptor	247
9.6	Calculation of helix length, the bending angles between two local helix axes, and the average number of residues per turn of the truncated CTD (1-99) and (108) α -Syn using HELANAL server	250
9.7	List of atom-atom interactions within the Truncated CTD α -Syn (1-99) interface from the ESBRI server	254
9.8	List of atom-atom interactions within the Truncated CTD α -Syn (1-108) interface from the ESBRI server	254
Chapter 10		
Table No.	Chapter 10	Page No.
10.1	Secondary Structural content of pY39, pS87 and pS129 α -Syn after the simulation time using YASARA software	272
10.2	Intermolecular Hydrogen bond analysis of membrane bound pY39 α -Syn during the MD simulation of 100 ns with membrane bilayer as acceptor and pY39 α -Syn as donor	279
10.3	Intermolecular Hydrogen bond analysis of membrane bound pY39 α -Syn during the MD simulation of 100 ns with pY39 α -Syn as acceptor and membrane bilayer as donor	280
10.4	Intermolecular Hydrogen bond analysis of membrane bound pS87 α -Syn during the MD simulation of 100 ns with membrane bilayer as acceptor and pS87 α -Syn as donor	281

List of Tables

10.5	Intermolecular Hydrogen bond analysis of membrane bound pS87 α -Syn during the MD simulation of 100 ns with pS87 α -Syn as acceptor and membrane bilayer as donor	282
10.6	Intermolecular Hydrogen bond analysis of membrane bound pS129 α -Syn during the MD simulation of 100 ns with membrane bilayer as acceptor and pS129 α -Syn as donor	284
10.7	Intermolecular Hydrogen bond analysis of membrane bound pS129 α -Syn during the MD simulation of 100 ns with pS129 α -Syn as acceptor and membrane bilayer as donor	285
10.8	List of atom-atom interactions within the pY39 interface from the ESBRI server	289
10.9	List of atom-atom interactions within the pS87 interface from the ESBRI server	290
10.10	List of atom-atom interactions within the pS129 interface from the ESBRI server	290

List of Abbreviations

Å	Angstrom
AD	Alzheimer's disease
α -Syn	Alpha Synuclein
AMBER	Assisted Model Building with Energy Refinement
BBB	Blood brain Barrier
BFE	Binding free energy
β -Syn	Beta Synuclein
CASTp	Computed Atlas of Surface Topography of proteins
CHARMM	Chemistry at HARvard Macromolecular Mechanics
CoM	Centre of Mass
COMT	catechol-O-methyl transferase
cryoEM	cryo-electron microscopy
1CSSI	one-character secondary structure information
CTD	C-Terminal domain
3-D	3-Dimensional
3DFFT	three-dimensional fast Fourier transform
CGenFF	CHARMM general force field
CPCM	conductor-like polarizable continuum model
CPPTRAJ	A rewrite of PTRAJ in C++
DBS	Deep Brain Stimulation
DFT	Density Functional theory
DLB	dementia with Lewy Bodies
DNA	Deoxyribonucleic Acid
DOPC	1,2-Dioleoyl-sn-glycero-3-phosphatidylcholine
DOPE	1,2-Dioleoyl-sn-glycero-3-phosphatidylethanolamine
DOPS	1,2-Dioleoyl-sn-glycero-3-phosphatidylserine
DSSP	Dictionary of Secondary Structure for Protein
ω	electrophilicity
EA	Electron affinity
EDP	Electron density profile
ELE	electrostatic energy
ESBRI	Evaluating the Salt BRIdges in Proteins
FEL	Free energy landscape
FFT	Fast Fourier Transform
FF99SB	Force-field 99 Stony Brook
γ -Syn	Gamma synuclein
GABA	gamma-aminobutyric acid
GAFF	General Amber force field

List of Abbreviations

GB	Generalized Born
GBSA	Generalized Born Surface Area
GUI	Graphical user interface
HOMO	highest occupied molecular orbitals
IDP	Intrinsically Disordered Protein
IDR	Intrinsically Disordered Regions
IP	ionization potential
kDa	kilo Dalton
LB	Lewy Bodies
LBD	Lewy Bodies disease
L-DOPA	L-3,4-dihydroxyphenylalanine
LHOP	local helix origin points
LN	Lewy neurites
LUMO	lowest unoccupied molecular orbitals
MAO	monoamine oxidase
MC	Monte Carlo
MD	Molecular Dynamics
MESP	molecular electrostatic potential map contour
MM	Molecular mechanics
MO	Molecular orbitals
MSA	multiple system atrophy
N	nucleophilicity
NAC	non-amyloid component
NBO	Natural bond orbital
NIH	National Institutes of Health
NMR	Nuclear Magnetic Resonance
NPT	constant-temperature, constant-pressure ensemble
ns	Nanosecond
NVT	constant volume
PBC	Periodic boundary conditions
PCA	Principal Component Analysis
PD	Parkinson's Disease
PDB	Protein Data Bank
PDD	PD Dementia
PDI	protein disulfide isomerase
PME	Particle Mesh Ewald
PPI	protein-protein interactions
ps	Picosecond
pS87	Phosphorylated at Serine 87

List of Abbreviations

pS129	Phosphorylated at Serine 129
PTM	Post Translational Modification
PTRAJ	Short for Process TRAJectory
pY39	Phosphorylated at Tyrosine 39
RBVI	Resource for Biocomputing, Visualisation, and Informatics
RCSB	Research Collaboratory for Structural Bioinformatics
R _g	Radius of Gyration
RMSD	Root Mean Square Deviation
RMSF	Root Mean Square Fluctuation
SA	Surface Area
SASA	Solvent-accessible surface area
SCF	Self-consistent field
SCOP	Structural Classification of Proteins
SDM	Site directed mutator
SOPMA	self-optimized prediction multiple alignment method
SVs	Synaptic vesicles
TCNE	tetracyanoethylene
TFE	trifluoroethanol
TIP3P	Transferable Intermolecular Potential Three-point
TIP4Pew	Transferable Intermolecular Potential four-point ewald
UCL	University College, London
UCSF	University of California, San Francisco
VDW	van der Waals contribution
VMD	Visual Molecular Dynamics
WHO	World Health Organization
WT	Wild Type

List of Publications

This thesis is partly based on the following original communications:

1. **Das, D.** and Mattaparthi, V.S.K. Computational investigation on the conformational dynamics of C-terminal truncated α -Synuclein bound to membrane. *Journal of Biomolecular Structure and Dynamics*, 2024. DOI: <https://doi.org/10.1080/07391102.2024.2310788>
2. **Das, D.**, Bharadwaz, P. and Mattaparthi, V.S.K. Computational investigations on the effect of the pepditomimetic inhibitors (NPT100-18A and NPT200-11) on the α -Synuclein and lipid membrane interactions. *Journal of Biomolecular Structure and Dynamics*, 2023. DOI: <https://doi.org/10.1080/07391102.2023.2262599>
3. **Das, D.** and Mattaparthi, V.S.K. Conformational dynamics of A30G α -Synuclein that causes familial parkinson disease. *Journal of Biomolecular Structure and Dynamics*, 2023. DOI: <https://doi.org/10.1080/07391102.2023.2193997>
4. **Das, D.**, Kakati, M., Gracy, A., Sanjeev, A., Patra, S.M., and Mattaparthi, V.S.K. Screening of druggable conformers of α -Synuclein using molecular dynamics simulation. *Biointerface Research in Applied Chemistry*, 10, 5338-5347, 2020. DOI: <https://doi.org/10.33263/BRIAC103.338347>
5. Kakati, M., **Das, D.**, Das, P., Sanjeev, A., and Mattaparthi, V.S.K. Effect of ethanol as molecular crowding agent on the conformational dynamics of α -Synuclein. *Letters in Applied NanoBioscience*, 9, 779-783, 2020. DOI: <https://doi.org/10.33263/LIANBS91.779783>

List of Publications

Other Publications:

1. Srivastava,V., Naik, B., Godara, P., **Das, D.**, Mattaparathi, V.S.K., and Prusty, D. Identification of FDA-approved drugs with triple targeting mode of action for the treatment of monkeypox: a high throughput virtual screening study. *Molecular Diversity*, 20, 1-15, 2023. DOI: <http://doi.org/10.1007/s11030-023-10636-4>
2. Yata, V.K., Dutta, N., **Das, D.**, and Mattaparathi, V.S.K. An In Silico Study for the Identification of Novel Putative compounds Against the Wild and Mutant Type Penicillin Binding Protein 2 of Neisseria Gonorrhoeae. *Biointerface Research in Applied Chemistry*, 11(2), 2020. DOI: <https://doi.org/10.33263/BRIAC112.89969006>
3. Yata, V.K., **Das, D.**, Deb, A., Das, N., Mahanta, G., Arora, B., and Mattaparathi, V.S.K. An In-Silico Study of Stable and Environment-Friendly Oryza sativa Urease. *Biointerface Research in Applied Chemistry*, 11(3), 2020. <https://doi.org/10.33263/BRIAC113.1023810247>
4. Das, C., **Das, D.**, and Mattaparathi, V.S.K. Computational Investigation on the Efficiency of Small Molecule Inhibitors Identified from Indian Spices against SARS-CoV-2 Mpro. *Biointerface Research in Applied Chemistry*, 13(3), 2023. <https://doi.org/10.33263/BRIAC133.235>
5. Das, C., Hazarika, P.J., Deb, A., Joshi,P., **Das, D.**, and Mattaparathi, V.S.K. Effect of Double Mutation (L452R and E484Q) in RBD of Spike Protein on its Interaction with ACE2 Receptor Protein. *Biointerface Research in Applied Chemistry*, 13(1), 2023. DOI: <http://doi.org/10.3390/vaccines11010023>
6. Dutta, M., Deb, A., **Das, D.**, and Mattaparathi, V.S.K. A Computational Approach to Understand the Interactions Stabilizing the A β 1-42 Oligomers. *Biointerface Research in Applied Chemistry*, 11(1), 2021. DOI: <https://doi.org/10.33263/BRIAC112.88048817>
7. Das, C., **Das, D.**, and Mattaparathi, V.S.K. Effect of Mutations in the SARS-CoV-2 Spike RBD Region of Delta and Delta-Plus Variants on its Interaction with ACE2 Receptor Protein. *Letters in Applied NanoBioscience*, 12(4), 2023. DOI: <https://doi.org/10.33263/LIABNS124.118>

In addition, this thesis also contain unpublished data.

1. **Das, D.**, and Mattaparthi, V.S.K. “Computational investigation on conformational ensembles of A30G α -Synuclein in its membrane bound state and in free solution that causes familial PD” National Seminar on “Excitements in Biological Research” held at Department of MBBT, Tezpur University on 6 th March, 2023. (Oral Presentation, 1st Prize).
2. **Das, D.**, and Mattaparthi, V.S.K. “Impact of phosphorylation at Ser87 on the α -Synuclein aggregation and synuclein-membrane interactions: an in silico study” in the National seminar "Research at the Interface of Chemical, Biological and Material Sciences” held at Department of Chemical Sciences, Tezpur University on 10th March, 2023. (Oral Presentation, 3rd prize)
3. **Das, D.**, and Mattaparthi, V.S.K. “Effect of pY39 Post-translational modification on the interactions between α -Synuclein and Lipid Membrane” the India-12th India-Japan Science and Technology Conclave: International Conference on Frontier Areas of Science and Technology (ICFAST-2022) held at the University of Hyderabad on September 09-10, 2022. (Poster Presentation)